PROTEINS: Structure, Function, and Genetics 19:183–198 (1994)

The Closed Conformation of a Highly Flexible Protein: The Structure of *E. coli* Adenylate Kinase With Bound AMP and AMPPNP*

Michael B. Berry,[1] Bill Meador,[1] Tim Bilderback,[2] Peng Liang,[2] Michael Glaser,[2] and George N. Phillips, Jr.[1]

[1]W.M. Keck Center for Computational Biology and Department of Biochemistry and Cell Biology, Rice University, Houston, Texas 77251-1892 and [2]Department of Biochemistry, University of Illinois, Urbana, Illinois 61801

ABSTRACT **The structure of *E. coli* adenylate kinase with bound AMP and AMPPNP at 2.0 Å resolution is presented. The protein crystallizes in space group *C*2 with two molecules in the asymmetric unit, and has been refined to an *R* factor of 20.1% and an R^{free} of 31.6%. In the present structure, the protein is in the closed (globular) form with the large flexible lid domain covering the AMPPNP molecule. Within the protein, AMP and AMPPNP, an ATP analog, occupy the AMP and ATP sites respectively, which had been suggested by the most recent crystal structure of *E. coli* adenylate kinase with Ap_5A bound (Müller and Schulz, 1992, ref. 1) and prior fluorescence studies (Liang et al., 1991, ref. 2). The binding of substrates and the positions of the active site residues are compared between the present structure and the *E. coli* adenylate kinase/Ap_5A structure. We failed to detect a peak in the density map corresponding to the Mg^{2+} ion which is required for catalysis, and its absence has been attributed to the use of ammonium sulfate in the crystallization solution. Finally, a comparison is made between the present structure and the structure of the heavy chain of muscle myosin.**

Key words: X-ray crystallography, R^{free}, ATP and AMP binding sites, Mg^{2+} coordination

INTRODUCTION

Adenylate kinases are small enzymes of approximately 20–26 kDa which function to determine the concentration of adenylate nucleotides by catalyzing the following reaction:

$$Mg^{2+}ATP + AMP \leftrightarrow Mg^{2+}ADP + ADP$$

The reaction requires the presence of Mg^{2+} for catalysis but not for nucleotide binding,[3] and the process of binding substrates to the protein is known to involve large domain movements,[4] as typical of kinases.

These proteins are interesting both as a model of kinase function and as examples of large domain movements in small macromolecules. Adenylate kinases lend themselves well as models of kinase function due to their small size (~200 residues) and relatively low level of complexity. Their reaction is also straightforward, being a simple S_N2-type phosphate transfer without a covalent enzyme bound intermediate.[5] Thus, structures of the adenylate kinase ternary complex present an opportunity to methodically analyze the role of various residues, as well as Mg^{2+}, in phosphate transfer reactions. In this regard, adenylate kinase is a good candidate for site-directed mutagenesis aimed at changing the dynamics of domain movement and catalysis.

Adenylate kinases undergo two large domain movements in the process of binding substrates (Figs. 1 and 2). The more minor of these occurs when part of the protein closes over bound AMP, a movement which covers ~8 Å.[6] Far more interesting is the movement of the large lid domain when it closes over the active site upon ATP binding. This domain moves ~30 Å and undergoes an 88° hinge bending rotation, movements which are enormous for such a small protein (Fig. 1).[6,7] The occurrence of these large domain shifts in adenylate kinases may help to improve our understanding of the mechanics of large scale protein motions in other larger phosphotransferase proteins such as muscle myosin. Moreover, the small size of these proteins may in the future allow them to be used for molecular dynamics simulations to actually visualize these motions as they occur in solution.

*The structure is listed as 1ANK in the Brookhaven Protein Data Bank.

Received November 19, 1993; revision accepted March 31, 1994.

Address reprint requests to George N. Phillips, Jr., Department of Biochemistry and Cell Biology, P.O. Box 1892, Rice University, Houston, TX 77251.

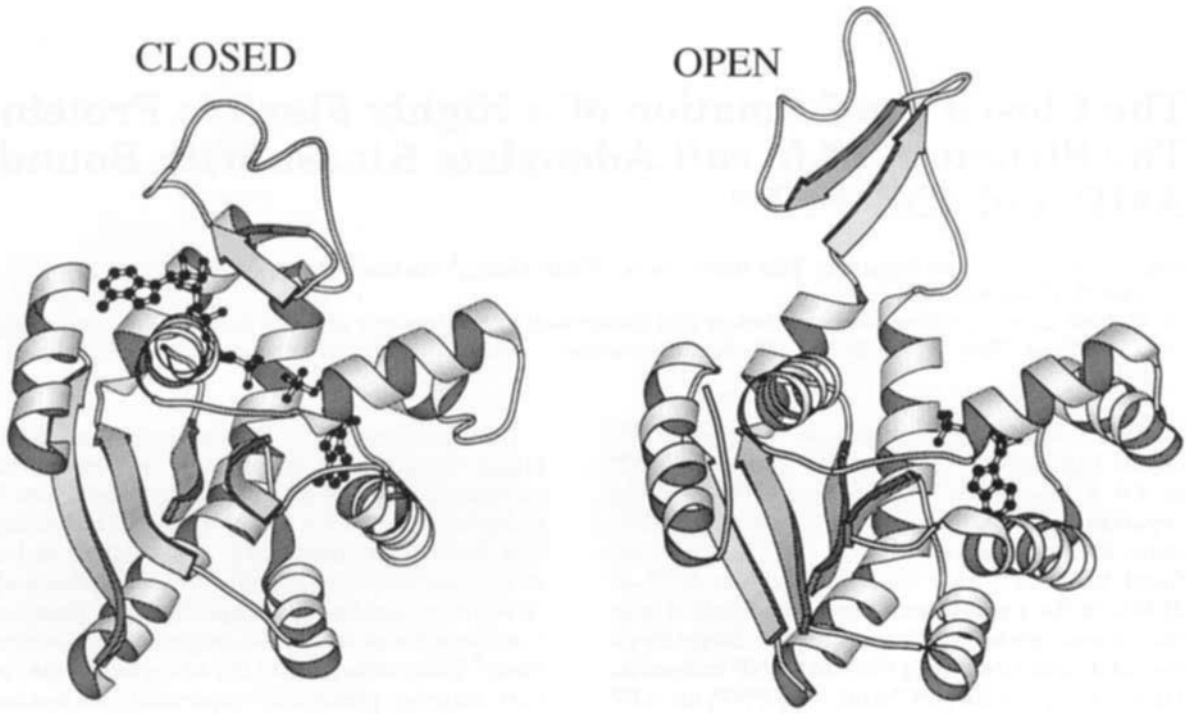

Fig. 1. The open and closed positions of the lid domain. The open and closed conformations of adenylate kinase are displayed. On the right in the open position is the structure of beef heart adenylate kinase with bound AMP[16] demonstrating the conformation of the protein prior to ATP binding. On the left is the structure presented in this paper with both AMP and AMPPNP bound demonstrating the ternary state of the enzyme.

Until recently, however, the location of substrate binding sites on the protein has been a subject of debate among the factions of X-ray crystallographers, spectroscopists, and molecular modelers. Determination of binding sites has been hampered by the fact that the initial structure determined by X-ray crystallography was that of the open form of the enzyme[8] with no bound substrate. In this state, it is not apparent where the substrates bind to the protein, and therefore, there have been numerous models based on X-ray,[9] NMR,[10,11] and molecular mechanics[12] experiments. It was not until the structure of the closed conformation of the enzyme was determined by X-ray crystallography[13] that the probable substrate binding sites on the protein could be inferred. Unfortunately, the determination of this form did not conclusively resolve the debate over the locations of these sites.

To date, three conformations of the enzyme have been determined by Schulz and co-workers using crystallographic methods: the unbound form,[8,14,15] the AMP bound form[16] (which revealed the location of the AMP site in a nonternary complex form), and the closed, pseudo-ternary form[1,13,17] with the bisubstrate analog Ap_5A bound. The cycle of conformational changes that the protein undergoes in the process of catalysis can be seen in Figure 2. Binding of substrate to either the ATP or AMP site is accompanied by a concomitant domain movement to enclose the bound substrate within the protein and to remove water from the region of phosphate transfer. Thus, of the structures Schulz and co-workers have been able to determine to date, the unbound form fits into Figure 2 category a, the AMP bound structure fits in Figure 2 category c, and the closed Ap_5A form is similar to Figure 2 category e. In an effort to confirm the model of the closed form of the enzyme (the Ap_5A form, Fig. 2e) as it was determined by Schulz and co-workers, we have solved the structure of adenylate kinase with both bound AMP and an ATP analog. The individual nucleotides bound to the protein in our structure provide a means of assessing the accuracy of the ATP and AMP binding sites which have been suggested by the structure of Ap_5A bound to the protein. Thus in the present paper, we present the structure of *E. coli* adenylate kinase with bound AMP and AMPPNP to reveal unambiguously the location of the sites of AMP and ATP binding.

METHODS

E. coli adenylate kinase was purified according to the methods of Althoff et al.,[18] and the protein was crystallized (at a concentration of 25 mg/ml) in 2.3 M ammonium sulfate/100 mM imidazole (pH 7.9) with 10 mM AMP, 10 mM AMPPNP, and 2 mM $MgCl_2$ by

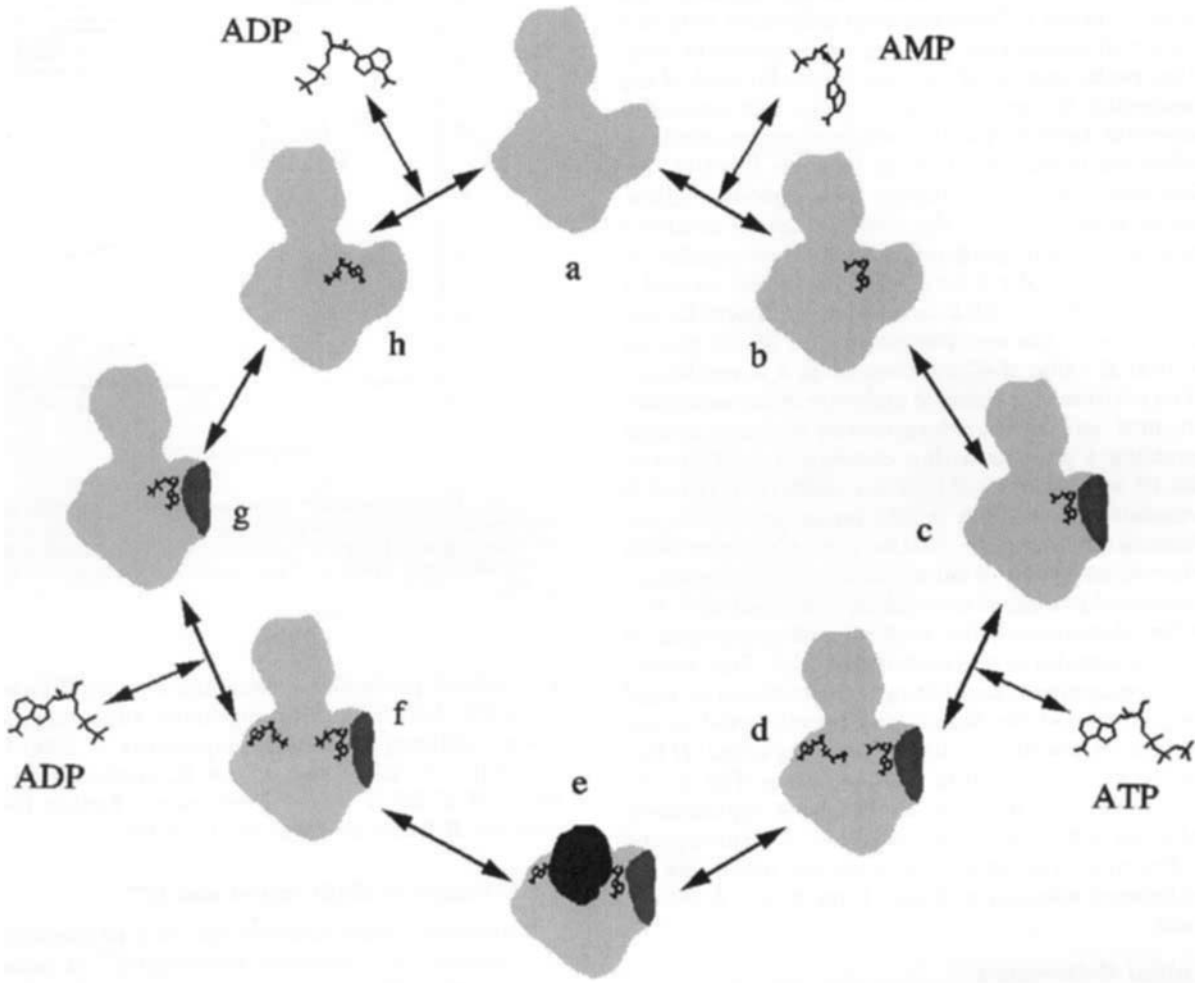

Fig. 2. Scheme of substrate binding to the protein. The series of protein conformational changes which are known or hypothesized to occur upon substrate binding are pictured. Substrates are shown binding first to the AMP site and then to the ATP site only for convenience of depiction (binding of nucleotides to the sites on the enzyme is of the random sequential type and thus can occur in either order). Darker shading indicates domain movement. (**a**) enzyme with no substrate bound.[15] (**b**) AMP loosely bound to the AMP site. (**c**) AMP tightly bound to AMP site with the AMP domain closed.[16] (**d**) ATP loosely bound to ATP site with the lid domain open, AMP bound within the closed AMP domain. (**e**) lid domain closed tightly upon nucleotide in ATP site, ternary complex (present structure). (**f**) ADP loosely bound to ATP site with the lid domain open, ADP bound within the closed AMP domain. (**g**) ADP tightly bound to AMP site within the closed AMP domain. (**h**) ADP loosely bound to the AMP site.

vapor diffusion methods. The crystals belong to space group $C2$ with two molecules in the asymmetric unit, and diffract to 2.0 Å. Unit cell parameters are a = 109.7 Å, b = 73.5 Å, c = 79.6 Å, $\alpha = \gamma =$ 90°, and β = 131.97°. Data sets were collected on both Siemens (Rice University) and San Diego Multiwire System area detectors (in the lab of Dr. Florante Quiocho, Baylor College of Medicine). The data set included 73,378 reflections, of which 30,135 were unique. The overall completeness of the data from 15 to 2 Å resolution is 85.3%.

All refinement was done using XPLOR.[19] Distance measurements and structural analysis were conducted using the CHAIN[20] and QUANTA programs. Figures were produced using MOLSCRIPT.[21]

Determination of the Position and Orientation of the Molecules Within the Asymmetric Unit

Attempts to determine the structure through the use of multiple isomorphous replacement methods proved to be successful only to about 4.5 Å resolution due to poor phasing. We were able to determine the rotation matrix between molecules in the asymmetric unit through the positions of UO_2 atoms in one derivative. However, the rotation matrix so produced was not accurate enough to allow symmetry averaging of the electron density to yield an interpretable result. A molecular replacement solution was found using the *E. coli* adenylate kinase/Ap_5A coordinates from Müller and Schulz.[1] Coordinates from one of the two molecules in the Ap_5A complex

(minus the substrate and solvent coordinates) were used to probe a Patterson map calculated with our observed intensities, yielding two significant rotation peaks (one set of rotation angles for each of the molecules in our asymmetric unit). The symmetry operator relating the two solutions was essentially identical to the relationship between the UO_2 ion locations found in multiple isomorphous replacement efforts. One of the rotation search solutions was used as a target function for a direct translation search in x and z directions. This search yielded a position (adk-1) with a correlation coefficient for one molecule in the asymmetric unit of 38.5% and an initial R value of 47.3% from 10 to 4 Å resolution. The position of the second molecule in our asymmetric unit (adk-2) was determined by the same process yielding a position with a correlation coefficient of 35.4% and an initial R factor of 48.5% from 10 to 4 Å resolution (Fig. 3). A third translation search was done to determine the relative y translation between the two molecules in our asymmetric unit, yielding a combined positional correlation coefficient of 70.0%. After determining the position and orientation of both molecules in our asymmetric unit, final molecular replacement positioning was conducted by rigid body fitting of the Müller and Schulz model to our data at extended resolution, producing a final R factor of 37.8% from 10 to 2 Å resolution (Fig. 3). At this point the multiple isomorphous replacement phasing efforts were discontinued. All subsequent refinement was conducted using the molecular replacement solution with data from 10 to 2 Å resolution.

Initial Refinement

Initial refinement began with a minimization of bad packing sterochemistry within the model structure, prior to refinement with the observed data. Geometry refinement yielded a structure with acceptable rms stereochemical deviations (rms bond length = 0.014 Å) for which the R factor was calculated to be 42.5%. Having produced a structure with acceptable sterochemistry, positional refinement was conducted with the inclusion of diffraction information, producing structures (adk-1 and adk-2) with an R factor of 32.9%. The two substrate molecules (AMPPNP and AMP) bound in our structure were seen clearly and manually fit to an $F_{obs}-F_{calc}$ difference map in both adk-1 and adk-2 (Fig. 4). Positioning the bound molecules was straightforward due to the high quality of the density surrounding the adenosine and phosphate moieties. AMP and AMPPNP atomic positions were then included in the structure, and the geometry of the model of the protein complexed with bound substrate molecules was refined (positional refinement without intensity data) to acceptable sterochemistry (rms bond length = 0.014 Å), and an R factor of 41.3% was determined for this model. The model was then positionally refined producing a structure with an R factor of 32.0%. Refinement by simulated annealing followed, utilizing an initial temperature of 3000 K, and steps of −25 K down to 300 K, producing an R factor of 27.3%. Positional refinement further lowered the R factor of the model to 26.8%.

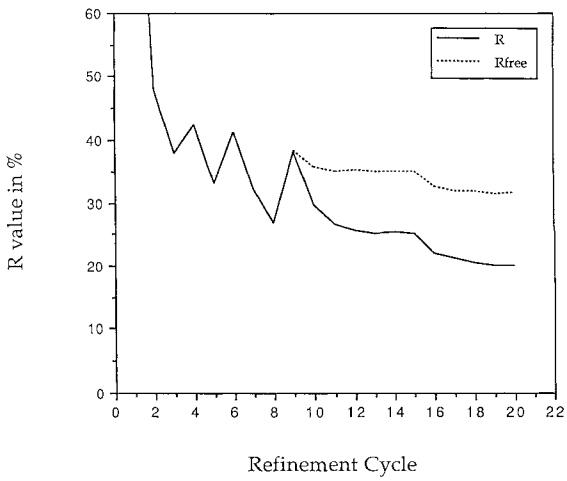

Fig. 3. Plot of R and R^{free} during molecular replacement and refinement. R and R^{free} are plotted versus the refinement cycle. R^{free} was measured after the model debiasing cycle through to the end of refinement. The final R was 20.1% and the final R^{free} was 31.6%.

Final Stages of Refinement and R^{free}

Statistical cross-validation can help in assessing the accuracy of structural refinement.[22] A small percentage, 10%, of the observed intensity data (called the reserved or test data) is randomly removed from the entire intensity data set, and is not used in the process of refinement. These reserved data are then used to calculate a special R factor, R^{free}, from the model produced by using the other 90% of the observed intensities (the working data). To remove any structural bias of the model for the reserved intensity data, our structure was scrambled by a short simulated annealing heating cycle (without intensity data), after which the model retains no "memory" of the reserved data. From this point, the standard R factor is calculated from the difference between the F_{calc} of the model and the F_{obs} of the remaining 90% of the intensity data (the working set). Likewise, R^{free} is calculated from the difference between the model F_{calc} and the F_{obs} of the reserved 10% of the data set (the test set). If the structure has been overfit to the working data, R^{free} will increase even as R decreases, while proper fitting results in a drop in both R and R^{free}.

Removal of the reserved data and model scrambling resulted in a R factor of 38.1% and an R^{free} of 38.2% (Fig. 3). After the debiasing dynamics run, positional refinement with the working set intensity

Fig. 4. Positive difference omit map showing substrate density. The density surrounding the AMP and AMPPNP molecules of adk-1 is illustrated. The figure was produced by computing a difference omit map of the structure minus the substrate molecules. Grid spacing of density map has been increased to improve visibility of AMP and AMPPNP molecules.

data yielded an R factor of 29.7% and an R^{free} of 35.7%. Temperature factors (B factors) were refined next, after which the R factor was 26.4% and R^{free} was 35.0%. Simulated annealing with a maximum temperature of 2000 K was used to help the model escape from any local minima in which it might still linger, after which R was 25.1% and R^{free} was 34.9%. At this point, we noted some bending of the adenine rings of our substrate molecules, and thus after reparameterizing and flattening the adenine rings, the structure underwent a third cycle of simulated annealing with a maximum temperature of 1000 K. The values of R and R^{free} following this cycle were 25.0 and 34.9%, respectively, and the rms deviation of bonds and angles were 0.019 Å and 2.35°.

Solvent positioning was done by location of significant peaks in an $F_{\text{obs}}-F_{\text{calc}}$ difference map. Water was fit by positional, B factor, and occupancy refinement in several steps at decreasing standard devia-

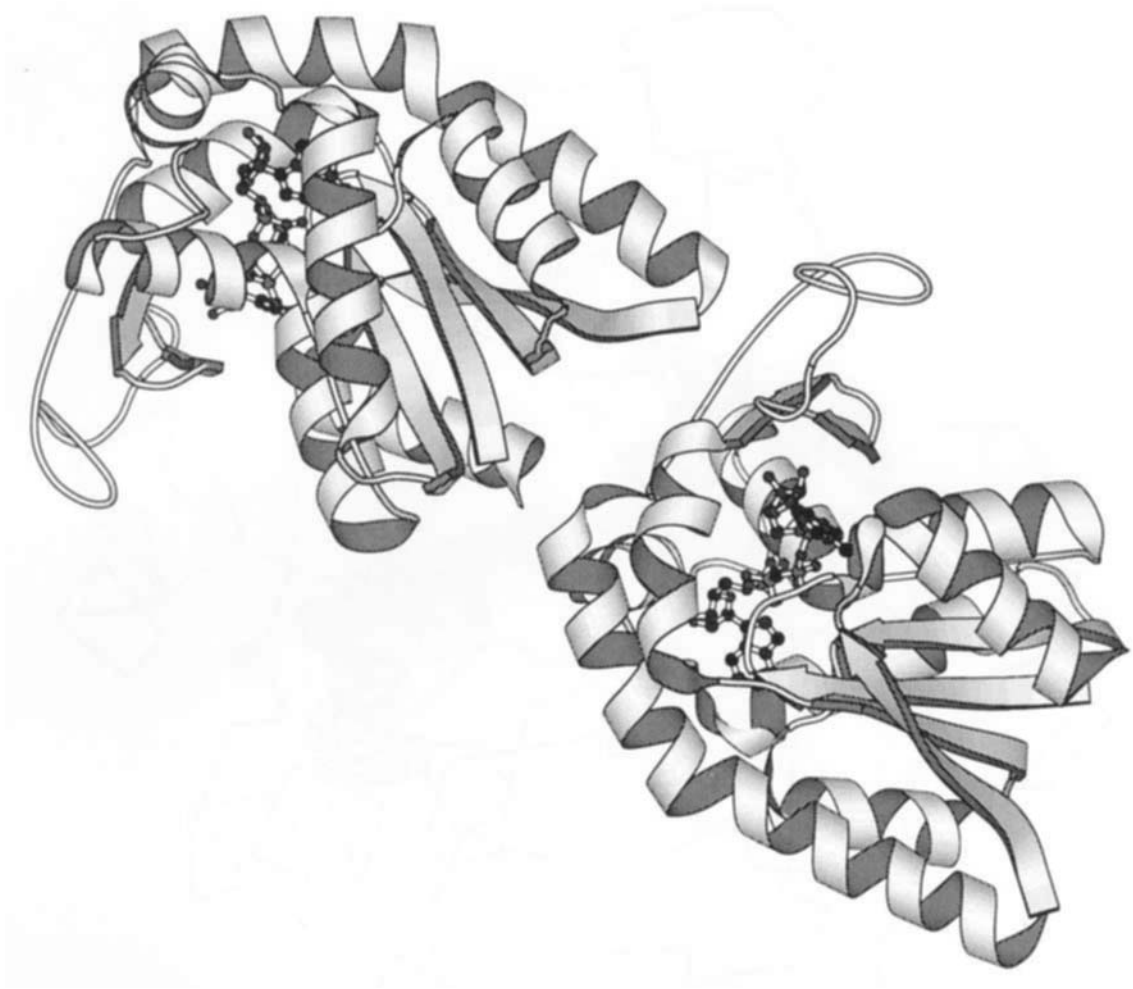

Fig. 5. The asymmetric unit of the crystal. The two molecules in the asymmetric unit related by a non-crystallographic 2-fold rotation are displayed. Contacts occur between the top of the lid domain in one molecule (adk-1, right) and the base of the immobile core of the other molecule (adk-2, left).

tion levels in the maps, from 4.0σ to 2.9σ. The R factor after the final water cycle (adk-1: 268 H_2O, adk-2: 265 H_2O) was 20.1%, while R^{free} was 31.6%. Solvent fitting was deemed complete when further addition of solvent molecules led to increases in R^{free}.

RESULTS

The overall tertiary structure and general organization of secondary structural elements in our structures of adenylate kinase with bound AMP and AMPPNP are very similar to those of the most recent *E. coli* adenylate kinase/Ap_5A structure.[1] The protein is in the closed form with bound nucleotides sandwiched between the mobile lid domain[6] (residues 115–163) and the relatively immobile core of the enzyme (Fig. 4). The closed lid fits closely to the protein core so that there is little exposure of the substrate and active site to the surrounding solvent. The two molecules in the asymmetric unit pack in a head to tail relationship, major contacts occurring on the top of the lid domain and the base of the immobile core of the two molecules (Fig. 5).

Structural comparison of the two molecules in our asymmetric unit with each other and with the prior high resolution *E. coli* adenylate kinase structures[1] (Figs. 6 and 7) illustrates the high degree of similarity between the structures. As measured with QUANTA, the average C_α rms deviation between the two molecules in our asymmetric unit is 0.52 Å, between the two molecules in the most recent *E. coli* adenylate kinase/Ap_5A structure it is 0.35 Å, and among all structures it is 0.48 Å. The average rms deviation of peptide backbone atoms between the two molecules in our asymmetric unit is 0.60 Å, in the *E. coli* adenylate kinase/Ap_5A structure it is 0.39 Å, and among all structures it is 0.56 Å. The average rms deviation of all atoms between the two molecules in our asymmetric unit is 1.45 Å, in the *E. coli* adenylate kinase/Ap_5A structure it is 0.63 Å,

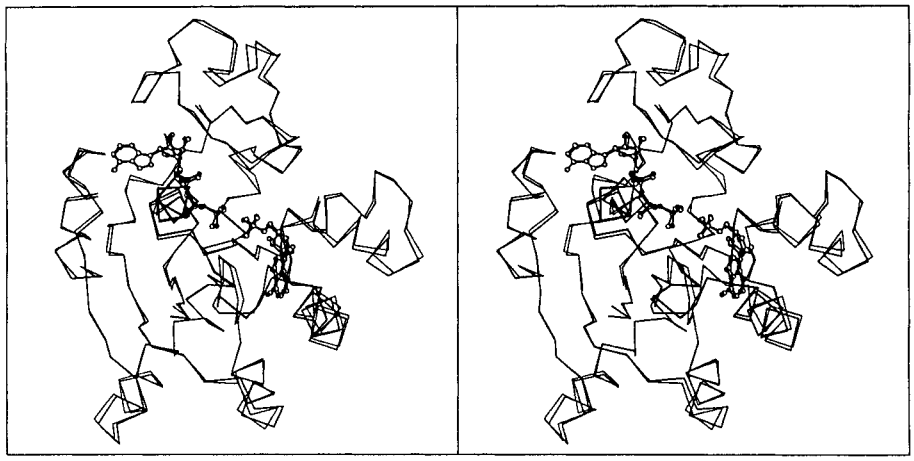

Fig. 6. Overlap of both molecules in the asymmetric unit. The overlap of the alpha carbon atoms of both protein molecules in the asymmetric unit and their substrates is shown. Thick lines are adk-1, thin lines adk-2. The rms deviation of the overlap of the alpha carbon atoms from both molecules in the asymmetric unit is 0.52 Å, and the peptide rms deviation is 0.60 Å.

and among all structures it is 0.91 Å. The greater overall differences in the rms deviation between the two molecules in our asymmetric unit as opposed to those in the *E. coli* adenylate kinase/Ap_5A asymmetric unit is not likely due to differences in temperature factors between the two molecules, as indicated both by the overall average of temperature factors for the backbone atoms of each (9.10 $Å^2$ for adk-1 and 8.70 $Å^2$ for adk-2) and by the plot of average backbone atom *B* factors at each residue (Fig. 8). As can be seen in Figure 8, the plots of the average temperature factor per residue in adk-1 and adk-2 are very similar, suggesting that the differences in the rms deviations between the two molecules in our asymmetric unit are probably due to crystal packing forces.

Structural Details of AMP and AMPPNP Binding

AMP and AMPPNP are bound with terminal phosphates facing each other in a roughly collinear arrangement spanning the protein beneath the closed lid domain (Figs. 4, 5, and 6). The α phosphate of AMP is skewed slightly from the linear phosphate chain arrangement, with one phosphate oxygen of AMP in close proximity to the γ phosphorous of AMPPNP (Fig. 9). Both nucleotides are oriented with extended phosphate chains, the riboses are in the $C_{2'}$-*endo* conformation for AMPPNP and the $C_{2'}$-*exo*–$C_{3'}$-*endo* conformation for AMP, and both of the adenine bases are bound in the *anti* configuration. AMP and AMPPNP bind in roughly the same locale that Ap_5A did in prior structures,[1,13,17] with some variation due to the lack of Ap_5A's unphysiological fifth bridging phosphate in our structure (Ap_5A phosphate four, Fig. 9).

The AMPPNP adenine moiety binds similarly in both molecules of the asymmetric unit between the carboxy-terminus helix (residues 194–214), the glycine loop/helix dipole region (residues 7–20), and part of the lid domain (residues 117–160). The AMPPNP adenine has only one hydrogen bond to the protein, that being between adenine N6 (notation of Saenger[23]) and the Lys-200 backbone carbonyl oxygen. The binding pocket for the adenine is formed by a sandwich between Arg-119 and the peptide backbone region from Pro-201 to Val-202.

The two molecules in the asymmetric unit show some differences in the hydrogen bonding patterns of the AMP adenine moiety. In adk-1, the AMP adenine moiety has two interactions with the protein that are within hydrogen bonding distance (<3.0 Å): adenine N7 to Thr-31 side chain hydroxyl (2.7 Å) and Val-59 peptide nitrogen to adenine N3 (2.9 Å). Weaker interactions that might represent hydrogen bonding are present between the adenine N6 to the Gly-85 backbone carbonyl oxygen (3.3 Å), the Gln-92 side chain carboxamide oxygen to the adenine N6 (3.1 Å), and the Gln-92 side chain carboxamide nitrogen to adenine N1 (3.1 Å). In adk-2, Val-59 peptide nitrogen to N3 at 2.8 Å is the only equivalent hydrogen bond to the binding of the AMP adenine in adk-1. Otherwise, the contacts which are out of hydrogen bonding range in adk-1 (N6 to the Gly-95 backbone carbonyl oxygen, and N1 to the Gln-92 side chain carboxamide nitrogen) are within hydrogen bonding distance in adk-2 (2.9 and 2.8 Å, respectively), and those that are within hydrogen bond distance in adk-1 (N7 to Thr-31 side chain hydroxyl at 2.7 Å) are much weakened (3.1 Å) in adk-2. The distance between the Gln-92 side chain carboxamide oxygen and adenine N6 also has increased to 3.3 Å, making the likelihood of a hydrogen bond unlikely. These alterations in the hydrogen bonding

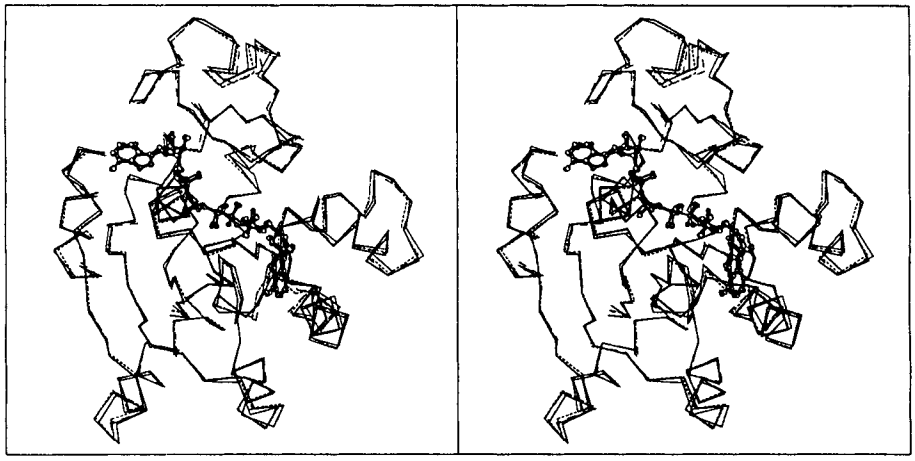

Fig. 7. Overlap of present structure with the structure of *E. coli* adenylate kinase with Ap_5A bound. The alpha carbon atoms of both molecules of the present structure with the bound substrates are overlapped with both molecules of the structure of *E. coli* adenylate kinase with Ap_5A bound.[1] Thick lines are adk-1, thin lines adk-2, dash and dot lines are the Müller and Schulz structures 1 and 2, respectively. Average rms deviation between the alpha carbon atoms of all four structures is 0.48.

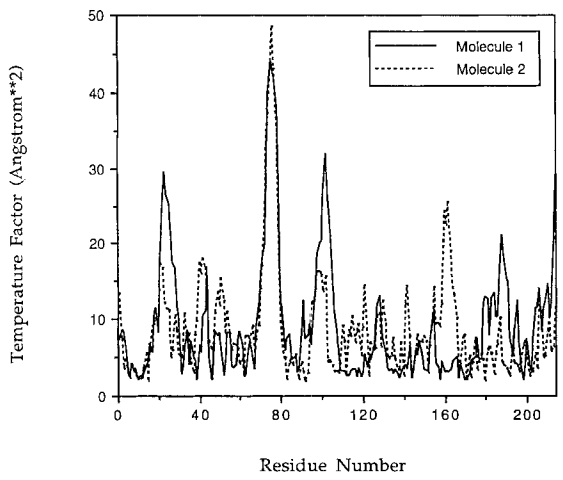

Fig. 8. Plot of average *B* factors for backbone atoms. Temperature factors for backbone C, O, N, and C_α atoms were averaged and plotted for both molecules in the asymmetric unit. Average for all the backbone atoms for each structure are near identical (9.10 $Å^2$ for adk-1, 8.70 $Å^2$ for adk-2).

patterns between the two molecules in the asymmetric unit appear to be caused primarily by movement of nearby Arg-88 (Fig. 10) to hydrogen bond (2.7 Å) to the Gly-85 backbone carbonyl oxygen displacing adenine N6 in adk-1, and this in turn causes close contacts between the head group of Arg-88 and adenine N7 (2.9 Å) which are not present in adk-2.

The ribose moieties of the substrates of both protein molecules in the asymmetric unit are similarly bound. The AMPPNP ribose moiety binds between the carboxy-terminus domain, the glycine loop/helix dipole, and the lid domain. The sugar is weakly bound, with one definite hydrogen bond to be found between the two molecules in the asymmetric unit (2.9 Å in adk-2, between the 2′ ribose hydroxyl and the Tyr-133 peptide carbonyl oxygen). The AMP ribose moiety binds within a region defined by residues 48–59 (part of the AMP binding domain). The sugar ring is bound to the protein by the 2′ and 3′ hydroxyls, the 2′ hydroxyl being within hydrogen bonding distance (2.8 and 2.7 Å in adk-1 and adk-2, respectively) of Lys-57 peptide carbonyl oxygen, and the 3′ hydroxyl being within hydrogen bonding of a water molecule, which is itself hydrogen bonded to one of the oxygens of the Asp-158 carboxylate (forming a bridge between protein and substrate).

Overlap of adk-1 and adk-2 demonstrates a high degree of similarity in the binding of the AMPPNP phosphate chains, with some variance in the binding of the AMP α phosphate (Fig. 9). Both the AMP and the AMPPNP phosphate chains have extensive protein contacts. In the closed position (as in our structure), the lid domain of *E. coli* adenylate kinase forms a highly charged pocket (occupied by the phosphate chains of both AMP and AMPPNP), between itself and main core of the protein. This pocket is lined with Arg-36, Arg-88, Arg-123, Arg-167, Lys-13, and Asp-84, as well as the anion hole[24]/helix dipole typical of glycine loops[25] (Figs. 11 and 12). The AMP α phosphate sits between the head groups of Arg-88 and Arg-36 (Fig. 10), and the AMPPNP phosphate chain is extended between the glycine loop (residues 7–14) and Arg-123 (Fig. 12). As will be discussed later, there is no density corresponding to the Mg^{2+} in association with the phosphate chain of AMPPNP.

The two molecules in the asymmetric unit, adk-1

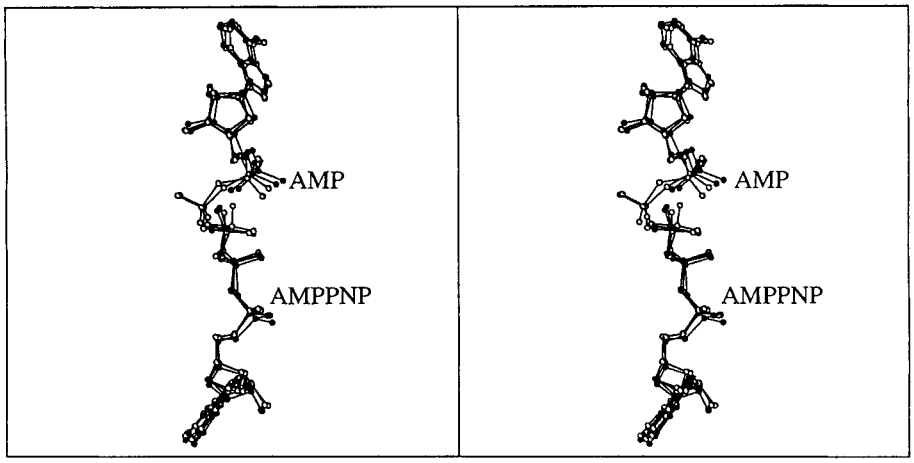

Fig. 9. Overlap of the bound molecules of the present structure and Ap_5A. The AMP and AMPPNP molecules from both molecules in the asymmetric unit (closed circles) are shown overlapped upon each other and upon the Ap_5A molecules (open circles) from the structure of *E. coli* adenylate kinase with Ap_5A bound.[1] Overlap was done using all atoms of the protein/substrate complex for both the present and Ap_5A structures, although only the bound molecules are pictured. The attacking AMP oxygen (α-O2) is closest to the γ phosphorous of AMPPNP.

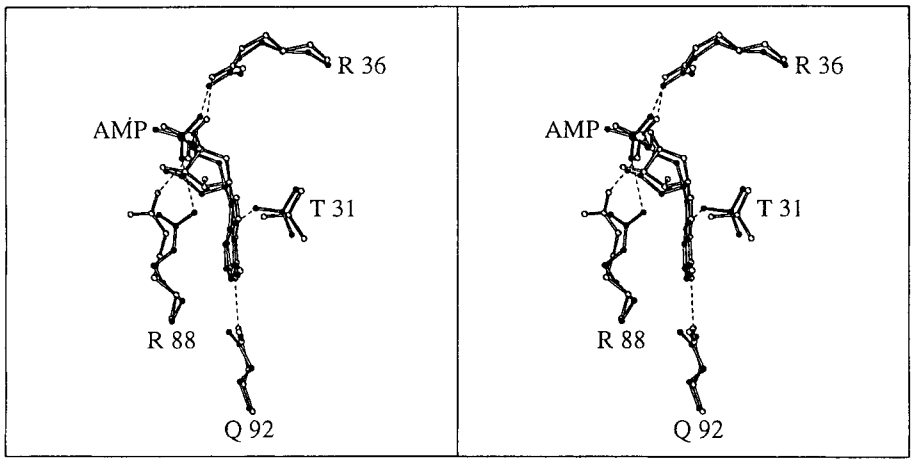

Fig. 10. Mobile residues in the AMP binding site. Pictured is AMP and four of the residues to which it hydrogen bonds from both molecules in the asymmetric unit. Residues and substrate from adk-1 have closed circles, those from adk-2 have open circles, and hydrogen bonds are displayed in dashed lines. Overlap between molecules in the asymmetric unit was done using all atoms. Variations in the positions of the AMP molecules and in the conformations or residues Thr-31, Gln-92, and Arg-88 result in different hydrogen bonding patterns for AMP between molecules in the asymmetric unit.

and adk-2, show some differences in the hydrogen bonding patterns of the phosphate moieties. In adk-1, α-O1 of the α phosphate of AMPPNP is within hydrogen bonding distance of the Thr-15 side chain hydroxyl and the Thr-15 peptide nitrogen (2.5 and 2.8 Å), and α-O2 is 2.8 Å from NH1 of the Arg-123 side chain head group (Fig. 12). In adk-2, the distances between α-O1 and the Thr-15 side chain hydroxyl/peptide nitrogen are 3.0 and 2.9 Å, and the interaction with Arg-123 NH1 is weak at 3.1 Å.

The β phosphate of AMPPNP has multiple interactions with the residues of the glycine loop. The β-O1 phosphate oxygen points downward into the center of the glycine loop, which in turn surrounds β-O1 and has the majority of its peptide amides pointed inward towards the phosphate oxygen (Fig. 12). In both adk-1 and adk-2, distances between the peptide nitrogens and the phosphate oxygen range from 3.0 to 4.2 Å. The Lys-13 side chain amino hydrogen bonds at 2.6 Å to the β-O1 oxygen in adk-1 and 2.9 Å in adk-2, and is also within hydrogen bonding distance of the Ala-8 peptide carbonyl oxygen (2.7 Å both molecules), thus forming a bridge between the phosphate chain of AMPPNP and the glycine loop. β-O2 interacts with the Gly-14 peptide nitrogen (2.9 Å in both molecules), and this phos-

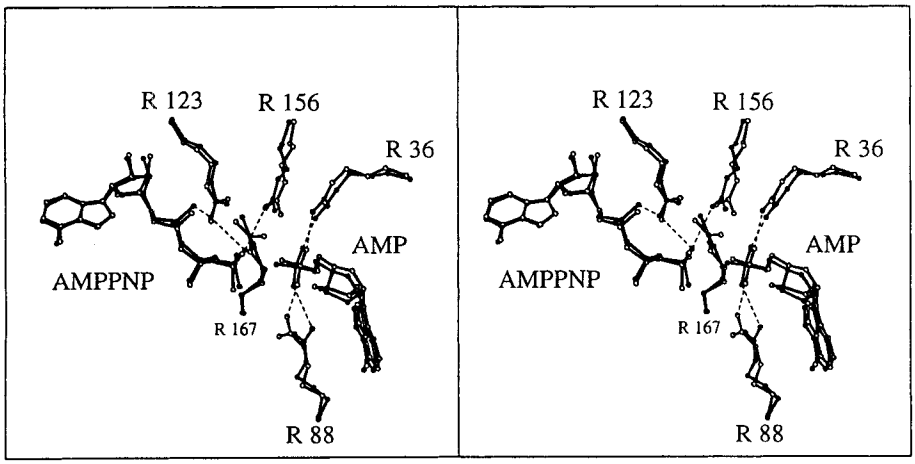

Fig. 11. Interactions of the active site arginines with bound molecules. The interactions between Arg-36, Arg-88, Arg-123, Arg-156, and Arg-167 and the bound substrates (AMP and AMPPNP) are pictured for both molecules in the asymmetric unit (adk-1 in closed circles, adk-2 in open circles, hydrogen bonds in dashed lines). Arg-36, Arg-123, Arg-156, AMP, and AMPPNP are roughly coplanar with the page, with Arg-88 above the plane of the page pointing inward from the foreground and Arg-167 behind the plane of the page pointing outward from the background. The front of the active site is above the page and the back is behind the page.

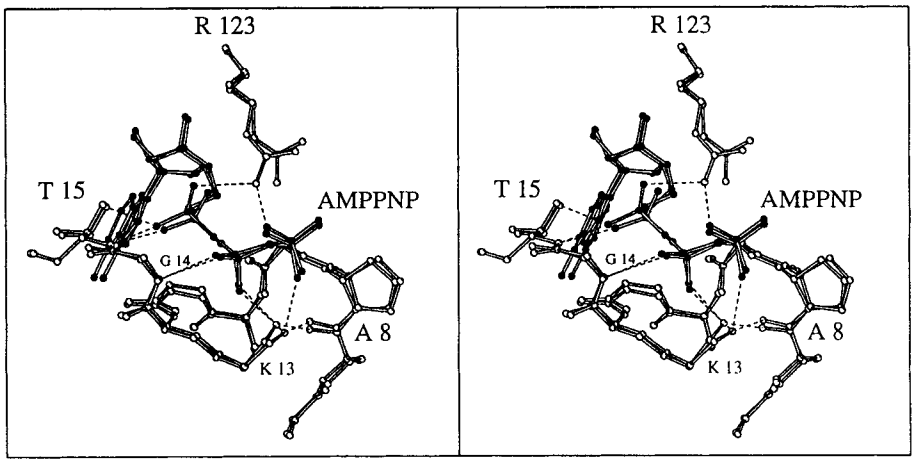

Fig. 12. The ATP binding site. AMPPNP, Arg-123, and residues 7–15 of the glycine loop from both molecules in the asymmetric unit (AMPPNP atoms in closed circles, protein atoms in open circles, hydrogen bonds in dashed lines) are depicted to illustrate the interactions between the protein and the phosphate chain of AMPPNP. The hydrogen bond bridge between Lys-13, Ala-8, and the β-O1 phosphate oxygen of AMPPNP is illustrated with dashed lines. Hydrogen bonds between α-O1 and Thr-15, and between β-O2 and Gly-14 are also depicted.

phate oxygen is positioned at the end of the helix formed by residues Gly-12 through Tyr-24 (at the positive end of the helix dipole). The nitrogen atom which bridges the β and γ phosphates of AMPPNP makes close contacts (possibly hydrogen bonds) with the side chain head group NH1 of Arg-123 (2.8 Å in both), and may also interact with the Gly-10 peptide nitrogen (2.9 Å in both). In both molecules, a water molecule bridges the gap between the β phosphate and the carboxylic acid head group of the Asp-84 side chain (Fig. 13), and helps to anchor the AMPPNP phosphate chain within the protein.

The γ phosphate has few obvious interactions with the residues of the active site in both molecules of the asymmetric unit. The γ-O3 phosphate oxygen, which points towards the opening of the active site cleft, is 3.0 Å from both the Arg-123 side chain head group NH1 and the Arg-156 head group NH1 in adk-1. In adk-2, the γ-O3 phosphate oxygen is out of hydrogen bonding distance to any residue except for the water bridging the gap between the phosphate chain and Asp-84 (Fig. 13). A bridging water is also present in this position in adk-1 (Fig. 13). The γ-O2 phosphate oxygen, which is oriented inwards towards the protein core, has only one contact with the protein, that being with the Lys-13 side chain amino

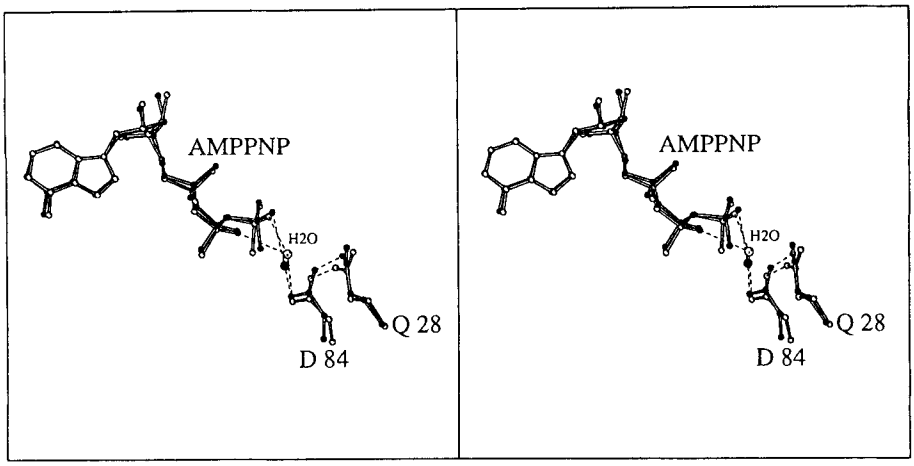

Fig. 13. Interactions between the AMPPNP phosphate chain and Asp-84. AMPPNP, Asp-84, Gln-28, and the bridging water (without hydrogens) are shown. Residues, water molecules, and substrate from adk-1 are in closed circles, those from adk-2 are in open circles, and hydrogen bonds are in dashed lines. In both molecules in the asymmetric unit, a water molecule forms a hydrogen bond bridge between Asp-84 and the O3 oxygen of the γ phosphate. In adk-2 the bridging water is also within hydrogen bonding distance of β-O2. Analysis of bond geometry indicates that the bridging water is not a Mg^{2+} ion.

at 3.1 and 2.8 Å in adk-1 and adk-2, respectably (Fig. 12). The γ-O1 phosphate oxygen points away from the opening of the active site cleft (towards Arg-167, Fig. 11), and has no interactions at less than 3.3 Å.

The α phosphate of AMP is poised for nucleophilic attack upon the γ phosphate of AMPPNP. α-O3, the α phosphate oxygen which is oriented to point towards the front of the active site cleft, hydrogen bonds with the Arg-36 side chain head group NH1 (2.6 Å adk-1, 2.8 Å adk-2) (Figs. 10 and 11). α-O2 points towards the back of the active site cleft and is not within hydrogen bond distance with any of the side chains within the active site (closest interactions with Arg-88 and Arg-156 head groups, ranging from 3.3 to 4.6 Å). However, α-O2 is angled so as to be in position to attack the γ phosphorous of AMPPNP (3.0 Å adk-1, 3.4 Å adk-2; Figure 9), and form the trigonal bipyramidal transition state characteristic of phosphate transfer.[26] α-O1 points inwards towards the core of the protein, and hydrogen bonds with the Arg-88 side chain head group NH1 (3.0 Å adk-1, 2.6 Å adk-2).

Orientation and Conformation of the Active Site Residues

The residues of the active site comprise two main types: positively charged residues involved in phosphate binding, orientation, transfer, and charge compensation (arginines 36, 88, 123, 156, 167, Lys-13, and the backbone amides of residues 7–14 comprising the glycine loop), and negatively charged/polar residues which are involved in arginine orientation and Mg^{2+} coordination (Asp-33, Asp-84, Asp-158, and Asp-159).

The active sites of adk-1 and adk-2 demonstrate some variability in the positioning of the five arginines which surround the AMP and AMPPNP phosphates, which is consistent with a flexible active site pocket. Viewed down the phosphate chain in both molecules, Arg-123, Arg-156, and Arg-36 stack in a coplanar arrangement (Fig. 11). (Arg-123 sits upon the AMPPNP phosphate chain; Arg-156, along with Arg-167, spans the gap between the terminal phosphates of AMP and AMPPNP; and Arg-36 sits upon the AMP α phosphate). The orientation of Arg-156 in adk-2 is different from that of adk-1, the side chain having moved back further into the pocket, due to the formation of a hydrogen bond between Arg-156 and Asp-158. Arginine-88, which rests against the opposite side of the α phosphate of AMP from Arg-36 (Fig. 10), has different orientations in adk-1 and adk-2, as well. In adk-1, Arg-88 is positioned so that both the head group NH1 and NH2 atoms can interact with one of the AMP phosphate oxygens, and the side chain NE can hydrogen bond with the Gly-85 peptide carbonyl oxygen. In adk-2, the head group is rotated so that only the NH1 is within hydrogen bond distance of the AMP α phosphate and Arg-88 NE is moved so as to be out of range to hydrogen bond with the Gly-85 peptide carbonyl oxygen. Arginine-167, which has its head group positioned halfway between the AMP α phosphate and the AMPPNP γ phosphate, has only one conformation in both adk-1 and adk-2.

Lysine-13 and the glycine loop (comprised of residues 7–14) are positioned so as to be in contact primarily with the β-O1 phosphate oxygen of AMPPNP, with a lesser degree of contact with one of the γ phosphate oxygens (γ-O2). As noted before, in

both adk-1 and adk-2 residues Gly-10 through Gly-14 form a semicircle about the β-O1 oxygen at distances generally outside that of hydrogen bonds (3.0 to 4.2 Å). The side chain of Lys-13 closes the circle surrounding the β-O1 oxygen (Fig. 12), and its headgroup amino forms a bridge between β-O1 and the Ala-8 peptide carbonyl by hydrogen bonding to each (2.8 and 2.6 Å, respectively). Residues 10 through 14 are oriented such that the peptide nitrogens point inwards towards the phosphate β-O1, presumably preventing charge repulsion by the peptide carbonyls, and to compensate the charge on the phosphate oxygen.

Negatively charged/polar active site residues are positioned so as to interact with the active site arginines. Two groups of negatively charged residues occur in the active site. One group comprises aspartates 158 and 159, and is located in the underside of the lid domain in the back of the active site pocket. The side chains of Asp-158 and Asp-159 orient the side chains of arginines 123, 156, and 167 by extensive hydrogen bonding networks. Asp-158 also helps to bind the AMP ribose by forming a hydrogen bond through an intermediate water to the 2′ ribose hydroxyl. Although there are variations between the orientations of the arginines in adk-1 and adk-2, the only difference in the hydrogen bonding of these residues to Asp-158 and Asp-159 is in the bond between the Asp-158 carboxylate OD1 and the Arg-156 head group NH1, which, as mentioned earlier, is absent in adk-1 due to movement of Arg-156 away from Asp-158.

The other negatively charged residues in the active site are located in the cavity between the AMP and AMPPNP phosphate chains and the opening of the active site pocket. Asp-33, Asp-84, and possibly Ser-30 comprise this group and are oriented so that their carbonyl and hydroxyl side chain oxygens point towards the phosphate chains of AMP and AMPPNP. There is a cavity in the active site between these residues and the phosphate chains, which may be present to allow room for Mg^{2+} coordination. Asp-84, which is in position to either coordinate directly to Mg^{2+}, or to the Mg^{2+} hydration sphere water molecules, forms a bridge via a water molecule to the AMPPNP phosphate chain in adk-1 and adk-2. The other side of Asp-84 is hydrogen bonded to Gln-28, forming a long hydrogen bonding chain from the β and γ phosphates of AMPPNP to the bridging water, from the bridging water molecule to Asp-84, and finally from Asp-84 to Gln-28 which is surface exposed (Fig. 13). Asp-33, a conserved residue among adenylate kinases, is at the front edge of the cavity, and points inwards towards the α phosphate of AMP from the mouth of the active site. Asp-33 may be responsible for the orientation of Arg-36 in regards to the AMP α phosphate, though the distances between Asp-33 and Arg-36 are not within hydrogen bonding range (3.8 and 3.4 Å in adk-1 and adk-2, respectively). It may be possible that Asp-33 plays some role in coordinating the hydration sphere of Mg^{2+}.

Magnesium in the Active Site

We expected that if magnesium were to be found within the structure, that it would bound between the β and γ phosphates of AMPPNP at distances of approximately 2.0 Å, and octahedrally coordinated with water molecules and the surrounding protein (Asp-84 in particular, ref. 27). However, we were unable to detect a peak in this region which would correspond to the specific stereochemistry of Mg^{2+}, despite the aforementioned Asp-84-to-βO1 bridging water molecules being in approximately the correct location (Fig. 13). Although it was tempting to think of this water as a potential Mg^{2+} ion, no evidence of a coordination sphere of water molecules could be detected in the density map, and, furthermore, both the bond angles and the bond distances between this peak and the AMPPNP phosphate chain were typical of water molecule hydrogen bonding rather than Mg^{2+} coordination.

DISCUSSION

Prior crystallographic assignment of the substrate binding sites[1,13] of adenylate kinase was done by comparison of the *E. coli* adenylate kinase/Ap_5A structure[1] to the structure of beef heart mitochondrial matrix adenylate kinase with bound AMP.[16] Comparison of the position of AMP in the beef heart structure with the position of the Ap_5A molecule in the *E. coli* structure allowed the assignment of the AMP binding site in the closed Ap_5A conformation of the protein, and by default, the remainder of the Ap_5A molecule (except for the extraneous phosphate 4) defined the ATP binding site. This assignment assumes that Ap_5A occupies both the ATP and the AMP sites. Our prior fluorescence studies agreed with the crystallographically assigned AMP binding site, but disagreed on the location of the ATP binding site.[2] Of question has been whether the binding of the Ap_5A molecule to the protein is analogous to AMP/ATP binding, and whether the protein is in a psuedo-transition state (the initial interpretation of the *E. coli* adenylate kinase/Ap_5A structure[17] reported a different lid conformation for the protein and differences in the positioning of the Ap_5A molecule relative to the most recent *E. coli* adenylate kinase/Ap_5A structure[1]).

Unambiguous verification of the assigned ATP and AMP binding sites in the closed conformation of the enzyme has been achieved by solving the structure of the complex of *E. coli* adenylate kinase with AMP and AMPPNP. AMPPNP differs from ATP only in possessing a phosphorous–nitrogen–phosphorous bond (as opposed to the phosphorous–oxygen–phosphorous bond of ATP) between the β and γ phosphates. The nitrogen atom serves as a poor leav-

ing group from the γ phosphorous, thus preventing loss or transfer of the γ phosphate. The presence of a nonhydrolyzable form (AMPPNP) of the phosphate donor (ATP), the normal phosphate acceptor (AMP), and Mg^{2+} in the crystallization solution was expected to allow crystallization of the enzyme in the transition state, that is, mimicking the high energy conformation just prior to catalysis of the reaction. Analysis of our structure has shown that both nucleotides, though not Mg^{2+}, are bound by the protein (Fig. 4).

In general, our structure is very similar to the most recent *E. coli* adenylate kinase/Ap_5A structure[1] in overall protein morphology (Fig. 7). As in the adenylate kinase/Ap_5A X-ray structures,[1,13,17] the present structure shows the enzyme to be in the closed conformation, assuming a much more globular shape than that seen in either the open[15] or the AMP bound[16] structures (Fig. 2a and c). In this conformation, the large mobile lid domain is rotated downward so as to seal the active site from the surrounding solvent (Fig. 2e), thus preventing phosphate hydrolysis.

The binding of AMP within our active site (Figs. 1, 4, and 6) confirms the AMP binding site determined based on the binding site determined based on the binding of Ap_5A to the protein[1,13,17] and on fluorescence data.[2] The binding of AMPPNP to the protein also confirms the ATP site assigned through analysis of the binding of Ap_5A.[1,13,17] The confirmation of the Ap_5A-assigned binding sites by the binding of AMP/AMPPNP (which, as separate nucleotides, have more degrees of binding freedom than the fused nucleotides of Ap_5A), suggests strongly that the most recent fluorescence (AMP site)[2] and crystallographically[1] assigned sites are the correct locations of ATP and AMP binding to the protein, and also supports the conclusion that the Ap_5A molecule is indeed a bisubstrate analog.[28] The AMP and ATP binding sites in the present structure differ considerably, however, from the positions assigned by NMR[10,11] and molecular mechanics.[12]

Comparison of the position of the phosphate chains of bound AMP and AMPPNP in the present structure with the equivalent portions of Ap_5A in the Müller and Schulz[1] structure suggests greater mobility for the phosphate of AMP relative to those of AMPPNP. The position of the AMP α phosphate in the two molecules of our structures shows some variability, and upon overlap with the Ap_5A structure, both α phosphates of our structure appear to be located closer to the mouth of the pocket than the corresponding portions of the Ap_5A molecule (Fig. 9). The differences in the positioning of the α phosphate of AMP and the equivalent phosphate of Ap_5A may be related to the bridging fourth phosphate of Ap_5A preventing the fifth phosphate (the α phosphate equivalent) from assuming the same conformation as seen in the present structure. The variations noted in the hydrogen bonding of the AMP adenine in the present structure may contribute to the variability in the position of the AMP α phosphate, and may reflect mobility of the nucleotide in the AMP site required for the α phosphate oxygen to move to attack the γ phosphate of AMPPNP.

The binding of AMPPNP (and its Ap_5A equivalent) shows a high degree of similarity between both molecules in the asymmetric unit in the conformation of the phosphate chain (Figs. 9, 12, and 13). The α and β phosphates have extensive hydrogen bonding networks to Arg-123 and the residues of the glycine loop, and show very similar binding between molecules in the asymmetric unit. The γ phosphate has few hydrogen bonds except to potentially mobile residues (Lys-13, possibly Arg-123 and Arg-156) facilitating its movement during phosphate transfer. The stability of the conformation of the γ phosphate between the two molecules in the asymmetric unit may be ascribed to the presence of the γ-O2 to Lys-13 to Ala-8 hydrogen bond bridge, and to the water bridge between γ-O3 and Asp-84, which bind the phosphate to the protein's internal surface. The water bridging Asp-84 and the β and γ phosphates is probably acting in a role similar to that which Mg^{2+} normally plays in stabilizing the phosphate chain.[27,29]

The apparent mobility of AMP and the apparent immobility of AMPPNP in the active sight lend support to a mechanism in which the AMP α phosphate changes position to attack the γ phosphate of AMPPNP. Interestingly, the separation between the attacking α phosphate oxygen of AMP and the γ phosphorous of AMPPNP differ between the two molecules in our asymmetric unit (3.0 Å in adk-1 and 3.4 Å in adk-2) suggesting a certain degree of conformational flexibility in the active site. This difference in separation between the attacking α phosphate oxygen and the γ phosphorous may result from crystal packing forces, although the equivalent atoms in the Müller and Schulz structure[1] (space group $P2_122_1$ rather than $C2$) have similar variability in separation (2.9 and 3.4 Å).

Residue positioning and general topology of the active site of the present structure shows a general similarity to the *E. coli* adenylate kinase/Ap_5A active site, although based on data from overlapping the structures, the present structure displays a higher degree of variability within the two molecules in the asymmetric unit than the *E. coli* adenylate kinase/Ap_5A structure. It is unclear whether the variations between molecules in the asymmetric unit in the conformations of the active site residues are due to different protein/substrate conformations, or to packing constraints affecting the active site. However, it is not surprising that the arginine residues, with their multiple roles in the adenylate kinase active site (charge compensation, transition state stabilization, phosphate transfer and orienta-

tion) and general flexibility as side chains, have different conformations between molecules in the asymmetric unit.

In our prior fluorescence work, we analyzed the mutation of several residues (Phe-86 → Trp, Tyr-133 → Trp, Tyr-133 → Cys, Leu-107 → Gln) for their role in substrate binding, based on changes in the K_m of AMP and/or ATP binding.[2] Having determined the structure in the present paper of the enzyme with both nucleotide binding sites occupied, it is possible to gain some understanding of the role the above mutations play in disrupting the binding characteristics of the protein. Mutation of Phe-86 to Trp led to a 44-fold increase in the K_m for AMP and caused a loss of AMP substrate inhibition. As has been described earlier,[1] Phe-86 is located in the core of the protein in close proximity to the adenine binding site of AMP. Thus, mutation of this residue to Trp is expected to distort the local topology of the AMP binding site preventing or decreasing the likelihood of the nucleotide adenine binding to the protein, thus resulting in an increase in K_m and the loss of AMP substrate inhibition.

Mutation of Tyr-133 to Trp does not greatly affect the kinetic behavior of the enzyme, which is consistent with the role Tyr-133 plays in the binding of AMPPNP. The substitution of Trp at this position may not significantly affect the position of the Tyr-133 carbonyl oxygen to which the 2′ ribose of AMPPNP binds, and the increase in the overall volume of the lid domain in this mutant does not significantly alter the K_m for ATP or the V_{max} of the reaction. This position is not entirely insensitive to substitution, however, as the mutation of Tyr-133 to Cys results in decreased activity and altered K_m values for ATP and AMP, likely due to large scale rearrangements of the mobile lid domain caused by the decrease in side chain volume.

The Leu-107 to Gln mutation was selected by its instability at high temperatures, a condition which suggests disruption in the packing of the hydrophobic core of the enzyme. The present structure has demonstrated that this residue is indeed buried within the enzyme core. Leu-107 is not in direct contact with the site of ATP binding in the present structure, and yet selectively affects the K_m for binding of ATP (and not AMP) and the V_{max} of the reaction. Alteration of Leu-107 to Gln probably disrupts the packing of Leu-5, Leu-82, and Phe-109 to which it is adjacent. Phe-109 and Leu-5 form a hydrophobic pocket under the glycine loop and the side chain of Lys-13, and thus this mutation may affect the role of Lys-13 and the glycine loop in binding the β and γ phosphates of ATP and in stabilizing the transition state of the reaction. This mutation may also disrupt the conformation of Leu-82, which may then displace Asp-84, preventing it from coordinating the Mg^{2+} ion bound to the nucleotide in the ATP site.[27] Lack of coordination of the Mg^{2+} would affect both the K_m of ATP and the V_{max} of the reaction.[27,29]

The Absence of Mg^{2+} in the Structure

Mg^{2+} has not been identified in either the present structure or in the *E. coli* adenylate kinase/Ap_5A structures,[1,17] although Mg^{2+} has been reported to be bound between the second and third phosphate of Ap_5A in complex with yeast adenylate kinase.[13] This position corresponds to binding between the β and γ phosphates of AMPPNP (or ATP), and is equivalent to the coordination of Mg^{2+} to GMPPNP as seen in the complex of the H-ras p21 protein with MgGMPPNP.[30] MgATP,[31] MgADP,[31] MgAMPPCP,[29] and $MgAp_5A$[27] have all been determined by NMR spectroscopy to complex with adenylate kinase in solution. Thus, it seems reasonable to suggest that the AMPPNP molecule should bind Mg^{2+} between the β and γ phosphates, although it is not seen in either our electron density maps or in the *E. coli* adenylate kinase/Ap_5A structures.

The explanation may be in the crystallization conditions. Previous crystal structures in which Mg^{2+} has been seen complexed to nucleotides have utilized PEG or PEP to crystallize the protein/nucleotide/ion complex.[13,30,32–35] Proteins crystallized in ammonium sulfate, the present structure included, have not demonstrated Mg^{2+} to be bound to the nucleotide[1,17], suggesting that ammonium sulfate competes with nucleotides for Mg^{2+} coordination in solution. The sulfate molecule could mimic free phosphate, coordinating the Mg^{2+} ion between two of the sulfate oxygen atoms, and this complex may then become insoluble. Although AMPPNP is expected to be preferred by Mg^{2+} for coordination, the more than 1000-fold difference in concentration between AMPPNP and ammonium sulfate in the crystallization mixture likely decreases the probability of Mg^{2+}/AMPPNP complexes in solution, as has been suggested in related studies.[36]

Structural Similarities to Muscle Myosin

The structure of adenylate kinase can be compared to the recently determined structure of muscle myosin.[24,37,38] Though greatly different in size and function, both proteins catalyze the transfer of a phosphate from ATP, suggesting that the two proteins may have similar nucleotide binding/active site regions. The sequence of the heavy chain of muscle myosin[39,40] does indeed have a glycine-rich region (residues 178–185) similar to that in adenylate kinases and other phosphotransferases.[41] In the myosin structure, this glycine-rich region forms a loop at the end of an α-helix (residues 178–200), creating a structure which is very similar to the helix dipole/glycine loop domain of adenylate kinases.[24] It is also apparent from the myosin structure that the conserved lysine (Lys-185) in the myosin glycine-rich loop is equivalent to *E. coli* ade-

nylate kinase Lys-13 in its glycine loop, and that the myosin Lys-185 is in a similar conformation to Lys-13 in the present structure. The topology of the region next to the glycine-rich loop in myosin suggests a Mg^{2+} binding fold with myosin Asp-463 equivalent to Asp-84 of *E. coli* adenylate kinase in the present structure. An aspartate or glutamate in this position is necessary for stabile coordination of the $Mg^{2+}(H_2O)_n$/ATP complex allowing the reaction to proceed to the pentacoordinate intermediate.

The myosin domain which sits directly over the glycine-rich loop (residues ~230–250) also shows similarities to adenylate kinases. This region of myosin contains several conserved positively charged residues including an arginine, suggesting an arrangement similar to the mobile portion of the *E. coli* adenylate kinase active site (the lid domain) wherein the arginines play roles in phosphate chain charge compensation and stabilization of the pentacoordinate intermediate. The positively charged residues of myosin may also play a role similar to that proposed[1] for the lid domain arginines of *E. coli* adenylate kinase, i.e., that of closing the domain on the bound nucleotide by way of charge attraction between the positively charged arginines and the negatively charged ATP phosphate chain. A large scale conformational change of this manner in myosin could play a role in ATP-dependent force production.

CONCLUSION

In summary, we have determined the 2.0 Å structure of *E. coli* adenylate kinase with bound AMP and AMPPNP, an ATP analog. Our protein, which crystallizes with two molecules in the asymmetric unit, demonstrates a higher degree of variability between residues in the active site than that seen in the prior high resolution *E. coli* adenylate kinase structure.[1] The positions of the nucleotides within our structure conclusively confirm the binding sites which had been suggested by recent crystallographic[1,13,16,17] and fluorescence[2] work. Furthermore, this structure adds another known step to the cycle of conformational changes (Fig. 2) adenylate kinase undergoes in the process of catalyzing its reaction, and provides a great deal of information on the mechanistics of kinase function in general. Moreover, we have been able to suggest a reason for the absence of Mg^{2+} from ours and other structures, and have noted similarities of the present structure to the nucleotide binding region of the heavy chain of muscle myosin.

ACKNOWLEDGMENTS

We acknowledge Michael Quillin, Anand Kolatkar, and Tod Romo for biochemical and computational discussions. We thank the Molecular Simulations Corporation for providing QUANTA. This work was supported by NIH grant AR32764 (GNP), the W.M. Keck Foundation, and NSF training grant BIR-9256580.

REFERENCES

1. Müller, C.W., Schulz, G.E. Structure of the complex between adenylate kinase from *Escherichia coli* and the inhibitor Ap_5A refined at 1.9 Å resolution. J. Mol. Biol. 224: 159–177, 1992.
2. Liang, P., Phillips, G.N., Glaser, M. Assignment of the nucleotide binding sites and the mechanism of substrate inhibition of *Escherichia coli* adenylate kinase. Proteins 9:28–36, 1991.
3. Vasavada, K.V., Kaplan, J.I., Nageswara Rao, B.D. Analysis of ^{31}P NMR spectra of enzyme-bound reactants and products of adenylate kinase using density matrix theory of chemical exchange. Biochemistry. 23:961–968, 1984.
4. Russel, P.J., Jr., Chinn, E., Williams, A., David-Dimarino, C., Taulane, J.P., Lopez, R. Evidence for conformers of rabbit muscle adenylate kinase. J. Biol. Chem. 265:11804–11809, 1990.
5. Fry, D.C., Kuby, S.A., Mildvan, A.S. NMR studies of the AMP-binding site and mechanism of adenylate kinase. Biochemistry 26:1645–1655, 1987.
6. Schulz, G.E., Müller, C.W., Diederichs, K. Induced-fit movements in adenylate kinases. J. Mol. Biol. 213:627–630, 1990.
7. Gerstein, M., Schulz, G., Chothia, C. Domain closure in adenylate kinase. Joints on either side of two helices close like neighboring fingers. J. Mol. Biol. 229:494–501, 1993.
8. Schulz, G.E., Biedermann, K., Kabsch, W., Schirmer, R.H. Low resolution structure of adenylate kinase. J. Mol. Biol. 80:857–864, 1973.
9. Pai, E., Sachsenheimer, W., Schirmer, R.H., Schulz, G.E. Substrate positions and induced-fit in crystalline adenylate kinase. J. Mol. Biol. 114:37–45, 1977.
10. Smith, G.M., Mildvan, A.S. Nuclear magnetic resonance studies of the nucleotide binding sites of porcine adenylate kinase. Biochemistry 21:6119–6123, 1982.
11. Fry, D.C., Kuby, S.A., Mildvan, A.S. NMR studies of the MgATP Binding site of adenylate kinase and of a 45-residue peptide fragment of the enzyme. Biochemistry 24: 4680–4694, 1985.
12. Caldwell, J.W., Kollman, P.A. Investigation of the substrate binding and phosphate transfer in adenylate kinase by molecular mechanics. Enzyme 39:61–77, 1988.
13. Egner, U., Tomasselli, A.G., Schulz, G.E. Structure of the complex of yeast adenylate kinase with the inhibitor P1,P5-di(adenosine-5′-)pentaphosphate at 2.6 Å resolution. J. Mol. Biol. 195:649–658, 1987.
14. Schulz, G.E., Elzinga, M., Marx, F., Schirmer, R.H. Three dimensional structure of adenyl kinase. Nature (London) 250:120–123, 1974.
15. Dreusicke, D., Karplus, P.A., Schulz, G.E. Refined structure of porcine cytosolic adenylate kinase at 2.1 Å resolution. J. Mol. Biol. 199:359–371, 1988.
16. Diederichs, K., Schulz, G.E. The refined structure of the complex between adenylate kinase from beef heart mitochondrial matrix and its substrate AMP at 1.85 Å resolution. J. Mol. Biol. 217:541–549, 1991.
17. Müller, C.W., Schulz, G.E. Structure of the complex of adenylate kinase from *Escherichia coli* with the inhibitor P1,P5-di(adenosine-5′-)pentaphosphate. J. Mol. Biol. 202: 909–912, 1988.
18. Althoff, S. Zambrowicz, B., Liang, P., Glaser, M., Phillips, G.N., Jr. Crystallization and preliminary X-ray analysis of *Escherichia coli* adenylate kinase. J. Mol. Biol. 199:665–666, 1988.
19. Brunger, A.T., Kuriyan, J., Karplus, M. Crystallographic R factor refinement by molecular dynamics. Science 235: 458–460, 1987.
20. Sack, J.S. CHAIN. J. Mol. Graph. 6:244–245, 1988.
21. Karulis, P.J. MOLSCRIPT: A program to produce both detailed and schematic plots of protein structures. J. Appl. Cryst. 24:946–950, 1991.
22. Brunger, A.T. Free R value: A novel statistical quantity for assessing the accuracy of crystal structures. Nature (London) 355:472–475, 1992.
23. Saenger, W. "Principles of Nucleic Acid Structure." New York: Springer-Verlag, 1984: 12.

24. Druesicke, D., Schulz, G.E. The glycine-rich loop of adenylate kinase forms a giant anion hole. FEBS 208:301–304, 1986.
25. Wierenga, R.K., De Maeyer, M.C.H., Hol, W.G.J. Interaction of pyrophosphate moieties with α-helixes in dinucleotide binding proteins. Biochemistry 24:1346–1357, 1985.
26. Cooperman, B.S. The role of divalent metal ions in phosphoryl and nucleotidyl transfer. Metal Ions Biol. Syst. 5:79–126, 1976.
27. Yan, H., Tsai, M-D. Mechanism of adenylate kinase. Demonstration of a functional relationship between aspartate 93 and Mg^{2+} by site directed mutagenesis and proton, phosphorous-31, and magnesium-25 NMR. Biochemistry 30:5539–5546, 1991.
28. Yan, H., Shi, Z., Tsai M-D. Mechanism of adenylate kinase. Structural and functional demonstration of arginine-138 as a key catalytic residue that cannot be replaced by lysine. Biochemistry 29:6385–6392, 1990.
29. Sanders, C.R. II, Tian, G., Tsai, M-D. Mechanism of adenylate kinase. Is there a relationship between local substrate dynamics, local binding energy, and the catalytic mechanism? Biochemistry 28:9028–9043, 1989.
30. Pai, E.F., Krengel, U., Petsko, G.A., Goody, R.S., Kabsch, W., Wittinghofer, A. Refined crystal structure of the triphosphate conformation of H-ras p21 at 1.35 Å resolution: Implications for the mechanism of GTP hydrolysis. EMBO 9:2351–2359, 1990.
31. Nageswara Rao, B.D., Cohn, M., Noda, L. Differentiation of nucleotide binding sites and role of metal ion in the adenylate kinase reaction by ^{31}P NMR. J. Biol. Chem. 253: 1149–1158, 1978.
32. Shirakihara, Y., Evans, P.R. Crystal structure of the complex of phosphofructokinase from *Escherichia coli* with its reaction products. J. Mol. Biol. 204:973–994, 1988.
33. Tong, L., de Vos, A.M., Milburn, M.V., Kim, S-H. Crystal structures at 2.2 Å resolution of the catalytic domains of normal ras protein and an oncogenic mutant complexed with GDP. J. Mol. Biol. 217:503–516, 1991.
34. Jancarik, J., de Vos, A., Kim, S-H., Miura, K., Ohtsuka, E., Noguchi, S., Nishimura, S. Crystallization of human c-H-ras oncogene products. J. Mol. Biol. 200:205–207, 1988.
35. Scherer, A., John, J., Linke, R., Goody, R.S., Wittinghofer, A., Pai, E.F., Holmes, K.C. Crystallization and preliminary X-ray analysis of the human c-H-ras-oncogene product p21 complexed with GTP analogues. J. Mol. Biol. 206: 257–259, 1989.
36. Rudolph, F.B., Fromm, H.J. Kinetic studies of adenosine 5′-triphosphatase activity of yeast hexokinase and its relationship to the mechanism of action of the enzyme. J. Biol. Chem. 245:4047–4052, 1970.
37. Walker, J.E., Saraste, M., Runswick, M.J., Gay, N.J. Distantly related sequences in the a- and b-subunits of ATP synthase, myosin, kinases and other ATP-requiring enzymes and a common nucleotide binding fold. EMBO. 1:945–951, 1982.
38. Rayment, I., Rypniewski, W.R., Schmidt-Bäse, K., Smith, R., Tomchick, D.R., Benning, M.M., Winkelmann, D.A., Wesenberg, G., Holden, H.M. Three-dimensional structure of myosin subfragment-1: A molecular motor. Science 261: 50–58, 1993.
39. Maita, T., Yajima, E., Nagata, S., Miyanishi, T., Nakayama, S., Matsuda, G. The primary structure of skeletal muscle myosin heavy chain: IV. Sequence of the rod, and the complete 1,938-residue sequence of the heavy chain. J. Biochem. 110:75–87, 1991.
40. Dibb, N.J., Maruyama, I.N., Krause, M., Karn, J. Sequence analysis of the complete *Caernorhabditis elegans* myosin heavy chain gene family. J. Mol. Biol. 205:603–613, 1989.
41. Saraste, M., Sibbald, P.R., Wittinghofer, A. The p-loop—a common motif in ATP- and GTP-binding proteins. TIBS 15:430–434, 1990.